ISSN 1069-3513, Izvestiya, Physics of the Solid Earth, 2015, Vol. 51, No. 3, pp. 354–361. © Pleiades Publishing, Ltd., 2015.
Original Russian Text © M.Yu. Reshetnyak, 2015, published in Fizika Zemli, 2015, No. 3, pp. 39–46.

Spatial Spectra of the Geomagnetic Field in the Observations and Geodynamo Models

M. Yu. Reshetnyak

Schmidt Institute of Physics of the Earth, Russian Academy of Sciences, ul. Bol'shaya Gruzinskaya 10, Moscow, 123995 Russia

e-mail: m.reshetnyak@gmail.com

Received April 5, 2014; in final form, June 6, 2014

Abstract—The correlation coefficients of the geomagnetic field on different spatial scales are estimated for the observations since 1590 and for a three-dimensional spherical-shell geodynamo model. It is shown that in the latter case, despite the presence of the geomagnetic reversals, the correlation of the magnetic field on different scales is low. The time behavior of the magnetic dipole is correlated to the evolution of the integral magnetic energy in the liquid core, whereas the dependence of the behavior of the integral kinetic energy on the magnetic field evolution is weak. Two-dimensional spectra of the magnetic field, velocity field, and cross-helicity in the liquid core of the Earth are presented.

Keywords: geodynamo, cyclonic turbulence, geomagnetic variations

DOI: 10.1134/S106935131503012X

INTRODUCTION

According to the contemporary understanding, the magnetic field of the Earth is generated by the dynamo mechanism in the liquid core (Roberts and King, 2013). Despite the fact that the magnetic field is quite ubiquitous in the Universe and extensively studied (Rüdiger et al., 2013), the investigation of the terrestrial and planetary dynamo has a series of specific features which manifest themselves in strong nonlinearity of the problem and extremely fast rotation of the planets. Moreover, the magnetic field observed on the surface of a planet (Hulot et al., 2010) only makes up a small fraction of the field inside the core and by its properties it only vaguely resembles the mean magnetic field in the region of its generation obtained after preliminary averaging.

Reproducing the magnetic field in a numerical model in such a way that it closely fits the observed field is, generally speaking, a statistical problem in the sense that on the longer timescales than the main geodynamo period (10 ka), the Gaussian coefficients in the Mauersberger spectrum (Mauersberger, 1956) are statistically independent (Hulot and Le Mouël, 1994; for more details, see the review (Khokhlov, 2012)). The absence of the correlation in the magnetic field on different scales turns out to have much in common with the processes occurring in the core considered as a turbulent system. Clearly, the archaeomagnetic view of secular variations as a system of the waves is only valid on the timescales that are somewhat longer than the periods of the waves themselves. This is supported by the wavelet analysis of the archaeomagentic data, which demonstrates the time evolution of the spectra (Burakov et al., 1998).

It is interesting that a linear relationship between the time period and spatial scale of the variations is also observed on the shorter periods of secular variation (60–500 yr) (Christensen and Tilgner, 2004), which could correspond to the weakly decaying turbulent magnetohydrodynamical (MHD) spectra in the liquid core. In this respect, the capabilities of numerical modeling become extremely helpful because testing the statistical independence of the Gaussian coefficients should be conducted on the long timescales where the observation accuracy becomes insufficient for assessing the evolution of the large wave numbers in the spectrum of the field. To be fair, we note that the paleomagnetic observations are unique in the sense that they provide extremely long time series of the large-scale characteristics of the magnetic field. As of now, such a long time series are unavailable in three-dimensional (3D) numerical modeling, which requires that the turbulent fields be resolved in the realistic range of the parameters and, thus, strongly increases the time of the computations (for more detail, see (Reshetnyak, 2013b)).

Below, by the example of a series of the known geomagnetic field databases, we will see how the estimates of the correlation between the Gaussian coefficients evolve with the increase in the length of the time interval. We will compare the results of analyzing the time

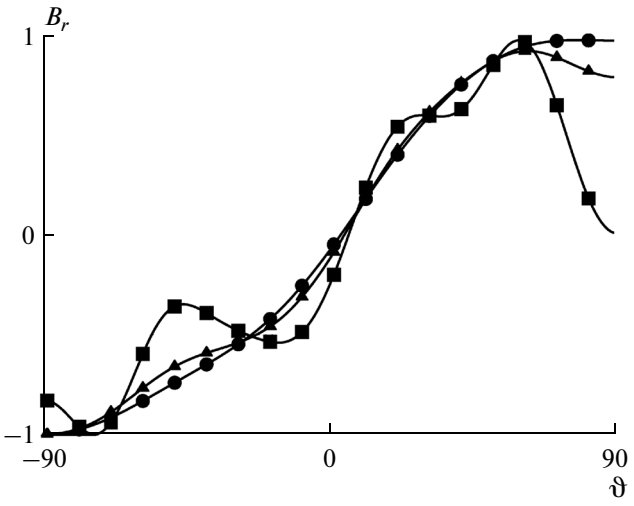

Fig. 1. The time- and latitude-average dependence of B_r on the latitude ϑ according to the IGRF-11 model for three radii: near the surface of the liquid core, $r = 3485$ km (the squares); in the middle of the mantle, $r = 4928$ km (the triangles); on the Earth's surface, $r = 6371$ km (the circles).

series containing a small number of the geomagnetic reversals, which were obtained in the 3D geodynamo models. We will also demonstrate, how and to what degree the characteristics of the geomagnetic field that are traditionally used in geomagnetism can help in studying the processes that occur in the liquid core of the Earth.

OBSERVATIONAL DATA. IGRF-11 AND GUFM1 MODELS

We consider the IGRF-11 geomagnetic field model which synthesizes the components of the geomagnetic field vector and the angular elements for the time interval from 1900 to 2012 (Finlay et al., 2010). The model incorporates the data from the observatories and satellites.

Figure 3 shows the radial B_r-component of the magnetic field for different distances from the liquid core of the Earth. In the first approximation, the geomagnetic field observed on the Earth's surface is the field of the dipole whose axis coincides with the rotational axis of the Earth and for which the radial component of the magnetic field has a simple dependence on latitude ϑ: $B_r = \cos(\vartheta)$. However, the dipole model only provides a coarse approximation, which does not allow for the higher order harmonics that still penetrate from the liquid core to the mantle. The extrapolation of B_r into the mantle's interior and onto the surface of the liquid core demonstrates the decrease in $|B_r|$ near the poles $|\vartheta| < \vartheta_{tc} \approx 60°$ (where index @[tc] denotes Taylor cylinder). We note that the projection of the Taylor cylinder (the cylinder that has a radius of the inner solid core of the Earth and the axis coinciding with the rotational axis of the Earth) onto the core/mantle boundary makes up 20.5° of the rotational axis. This decrease in the magnetic field in the high latitudes becomes quite understandable if we take into account that the main generation of the magnetic

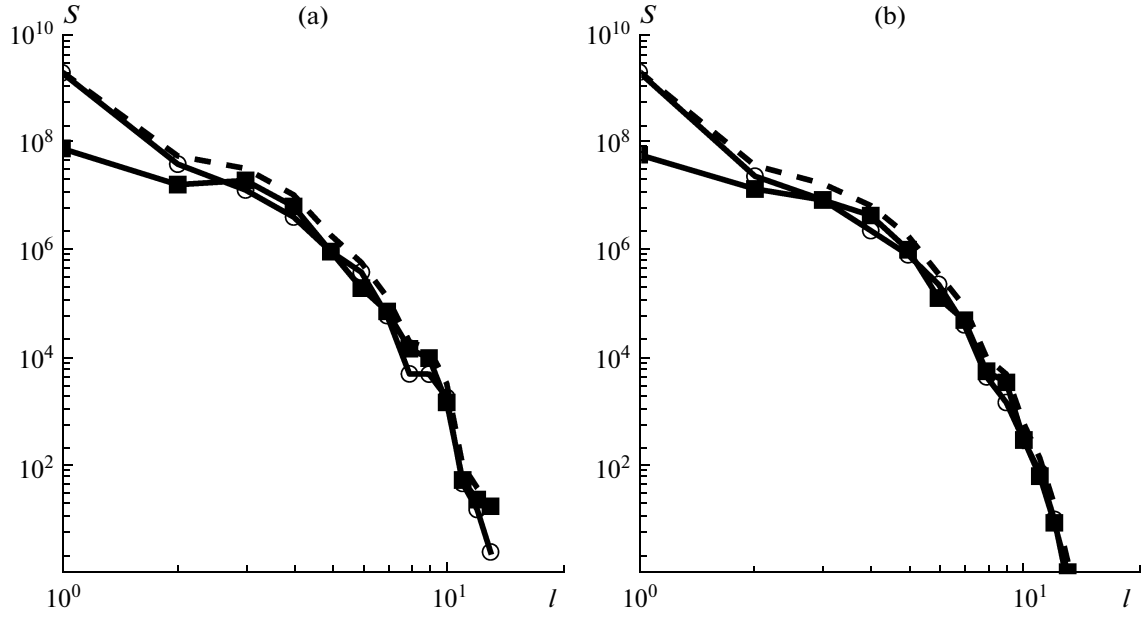

Fig. 2. The spectrum of the geomagnetic field for the (a) IGRF-11 model and (b) GUFM1 model. The line with squares, with circles, and dashed line show the antisymmetric part, symmetric part, and their sum, respectively.

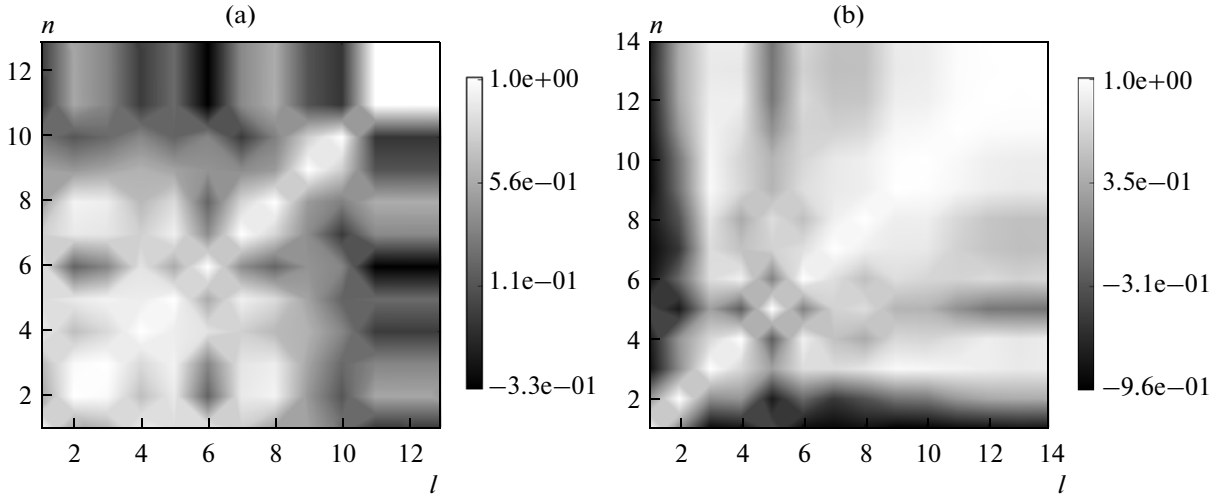

Fig. 3. The correlation coefficient r_{ln} for (a) IGRF-11 and (b) GUFM1 models.

field is due to the cyclones, which also have a certain scale near the Taylor cylinder.

For analyzing the energy characteristics, it is useful to consider the spectrum of the magnetic field (Mauersberger, 1956; Lowes, 1966):

$$S_l = (l+1)\sum_{m=0}^{l}\left(g_{lm}^2 + h_{lm}^2\right). \quad (1)$$

The Gaussian coefficients g_{lm} and h_{lm}, which are present in the expansion of the potential field in the spherical functions S_l^m (e.g., see (Parkinson, 1983)), can be grouped by the type of the symmetry with respect to the equatorial plane. For the dipole (antisymmetric) component, $l - m$ is odd, and for the symmetric component $l - m$ is even (Hulot and Bouligand, 2005). Figure 2a shows the full spectrum and its decomposition into the even and odd components. The dipole component is predominant. On the whole, the even and odd components have a similar saw-tooth structure, therefore the sign of their difference changes when l increases by unity.

Returning to the estimates of the correlation between the Gaussian coefficients, we reduce this problem to the question of the correlation between the values S_l and consider the correlation coefficient in the following form:

$$r_{ln} = \frac{\overline{(S_l - \overline{S_l})\cdot(S_n - \overline{S_n})}}{\sqrt{\overline{(S_l - \overline{S_l})^2}\cdot\overline{(S_n - \overline{S_n})^2}}}. \quad (2)$$

Record (2) differs from that suggested in (Bouligand et al., 2005), where the authors calculated the correlation between the Gaussian coefficients themselves; however, this formula significantly reduces the amount of the computations. The distribution function of r_{ln} is symmetric with respect to indices (l, n). For the random g_{ln} and h_{ln}, matrix r_{ln} is a unit matrix.

The correlation coefficient for the IGRF-11 model is illustrated in Fig. 3a. Except for the rather diffuse maximum near $l = n$, which corresponds to the autocorrelation, any other characteristic features are not observed in the behavior of r_{ln}. The existence of the correlation for the off-diagonal elements is due to the fact that the characteristic times of the variations in the field, τ_n,

$$\tau_n \frac{\sum_{m=0}^{l}\left(g_{lm}^2 + h_{lm}^2\right)}{\sum_{m=0}^{l}\left(\dot{g}_{lm}^2 + \dot{h}_{lm}^2\right)} \quad (3)$$

on the time interval from 1840 to 1990 are longer than the time interval covered by the IGRF-11 model (~100 yr). Here, $\dot{g}$ denotes the time derivative of g. It is known that τ_n obeys the following empirical law: $\tau_n = \tau_{sv}/n$ (Christensen and Tilgner, 2004), where $\tau_{sv} = 535$ yr and the number of the spherical function lies in the interval $n = 2, ..., 8$, which corresponds to the longer characteristic times than the observation time in the IGRF-11 model.

Consider the changes that occur when passing to the longer time series of the observed geomagnetic field. For doing this, we apply the GUFM1 model (Jackson et al., 2000), which is also suitable for synthesizing the magnetic field, and use the tabulated Gaussian coefficients since 1590. The model is based on the information retrieved from the records in the ship log books.

The spatial spectrum of the magnetic field (Fig. 2b) barely has any noticeable distinctions from the spectrum for the IGRF-11 model (Fig. 2a).

The correlation coefficient shown in Fig, 3b, besides the high diagonal correlation, also has areas of high negative correlation for $n = 1$, $l > 1$ (and for $l = 1$, $n > 1$), which could correspond to the energy redistribution between the dipole and higher harmonics during the secular variations of the magnetic field.

We see that for both the IGRF-11 and GUGM1 models, due to the finite length of the time series, the correlation coefficient r_{ln} is far from that predicted by the statistical theory.

Consider now the estimates yielded by the analysis of the simulated series, which are synthesized in the 3D dynamo models and contain a certain number of magnetic reversals.

THE DYNAMO MODEL

Modeling the geodynamo processes is a rapidly developing field in geophysics (Roberts and King, 2013). To date, a wide range of the models allowing for the compressibility of the liquid core, rotation of the solid core, and heterogeneities at the core/mantle boundary have been suggested. However, an excessive particularization of the models is barely justified because a number of the key parameters used in the numerical models for determining the planetary rotation velocity and the amplitude of the sources of energy and dissipation in the system are still far from the plausible geophysical values. Even for the dynamo model based on the simplest thermal convection scenario in the Boussinesq approximation, many of these parameters at best only provide an approach to the asymptotic regime corresponding to the dynamo in the Earth's core (Reshetnyak, 2013a).

Below, we consider the evolutional time series generated for the same set of the parameters as in the last example cited in (Reshetnyak, 2013a). We note that in this model, the convection of the conductive liquid in a rotating spherical shell with the radii $r = 0.35$ and 1 is driven by heating from below. The flows are cyclonic and highly geostrophic; they have nonzero average hydrodynamic helicity in the both hemispheres, which enables generation of a large-scale magnetic field. The simulations were carried out with the Rayleigh number $\mathrm{Ra} = 400$, Ekman number $\mathrm{E} = 2 \times 10^{-4}$, Prandtl number $\mathrm{Pr} = 1$, and Roberts number $\mathrm{q} = 7$. In the computations we used the pseudospectral code which implies decomposition of the vector fields into the poloidal and toroidal modes and subsequent expansion in the spherical functions and Chebyshev's polynomials. The computations were conducted on the supercomputing clusters of the Joint Supercomputer Center of the Russian Academy of Sciences (JSCC RAS) and Chebyshev cluster of the Moscow State University on 128^3 grids.

We begin considering the model time series from analyzing the evolution of the magnetic field at the core/mantle boundary. The characteristic scale unit of the diffusion time corresponds to 160 ka. The graphs in Figs. 4a and 4c show a few clearly expressed reversals of the magnetic field and the time intervals when the magnetic dipole g_1^0 has a low amplitude and is located in the low latitudes with nearly zero inclination I. The reversals mainly occur at the decreased magnetic energy and intensity of the magnetic field F.

Since the magnetic reversals are by definition associated with the reduction in the dipole (odd) component of the magnetic field, let us check whether the reversal process is accompanied by the change in the symmetry type of the total magnetic field on the surface. For doing this, as previously, we separate the magnetic energy into two components with odd and even $l - m$ (see Figs. 4 d, 4e). The calculations show that the both curves have a similar structure. For more clarity, we introduce the parity parameter

$$P = \frac{E^A - E^S}{E^A + E^S}, \tag{4}$$

which has a value of $+1$ for the energy that is antisymmetric relative to the equator and -1 for symmetric energy. Parameter P does not change significantly during the magnetic reversal (Fig. 4f). This is yet another argument supporting our hypothesis that the magnetic reversal insignificantly affects the dynamo process in the core overall.

The dynamo interval considered in the model, $\sim 4 \times 10^5$ yr, is by three orders of magnitude longer than the characteristic time of the variations τ_{sv}, which means that when calculating r_{ln}, we may expect to reveal a weak correlation between the Gaussian coefficients, if this correlation exists.

The correlation coefficient r_{ln} for the model time series (Fig. 5) has a distinct diagonal structure just as in the case without the reversals considered in (Bouligand et al., 2005). The unity values on the diagonal correspond to the autocorrelation estimates. The correlation between the values of S_l on the different scales ($l \neq n$) is very insignificant, as predicted in (Hulot and Le Mouël, 1994).

As we can see, the correlation between the magnetic dipole and the MHD characteristics of the system on the surface of the liquid core is very low. The correlation between the process of the magnetic field reversals and the characteristics averaged over the volume of the liquid core is even weaker. Figure 6 shows the volume-average kinetic and magnetic energies. It is clearly seen that the long-period magnetic variations are not observed in the time evolution of the volume-

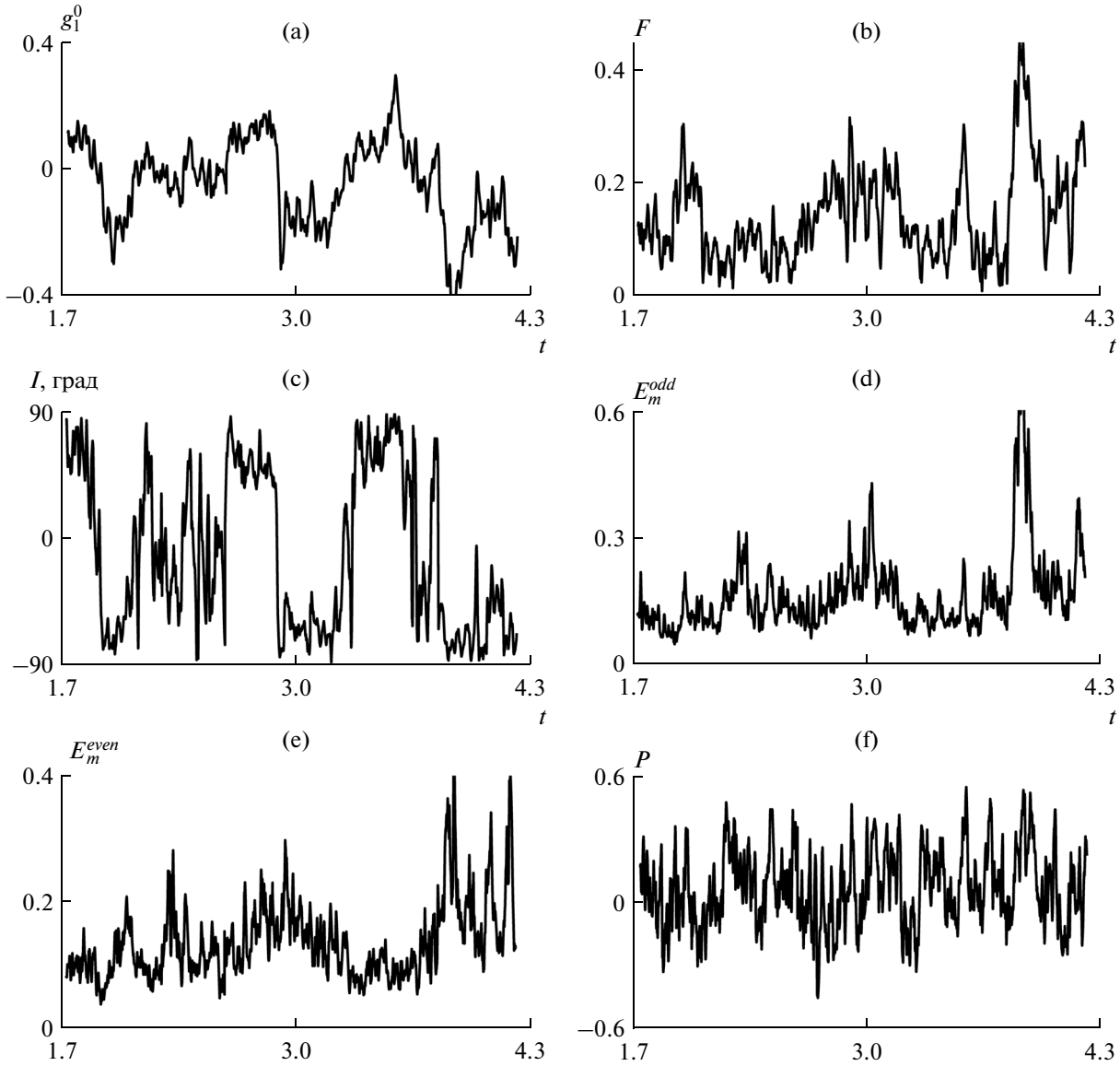

Fig. 4. The evolution of the (a) axisymmetric dipole, (b) magnetic field intensity, (c) inclination, (d) odd and (e) even magnetic energy, and (f) parity.

average kinetic energy. This reflects the fact that, although the amplitude of the magnetic energy is high, the field is force-free and it weakly affects the flows. A certain correlation is observed between the behavior of the volume-average magnetic energy and the intensity of the magnetic dipole. According to this, we should expect a low correlation between the velocity field and magnetic field, which is indeed demonstrated by the calculations (Fig. 6c). The correlation between the velocity field and magnetic field has its own name: it is referred to as the cross-helicity. It is invariant for the MHD equations in the absence of the external forces and dissipation (Woltjer, 1958). It can be shown that the presence of non-zero cross-helicity means the existence of a preferred polarity of the magnetic field. We note that this asymmetry is not factored in the system of the induction equations and Navier-Stokes equations, in which the magnetic force is quadratic with respect to the magnetic field, i.e. independent of its sign.

The different behavior of the magnetic and kinetic energies is closely associated with the different structure of the spectra of **V** and **B**. We introduce two-dimensional (2D) spectra of the velocity field $S_v(l,m) = \int_{r_\circ}^{r_1} \mathbf{V}^2 r^2 dr$, magnetic field $S_b(l,m) = \int_{r_\circ}^{r_1} \mathbf{B}^2 r^2 dr$, and cross-helicity $S_{vb}(l,m) = \int_{r_\circ}^{r_1} \mathbf{VB} r^2 dr$. Note that due to the geostrophic balance of forces, the kinetic energy is dominated by the harmonics

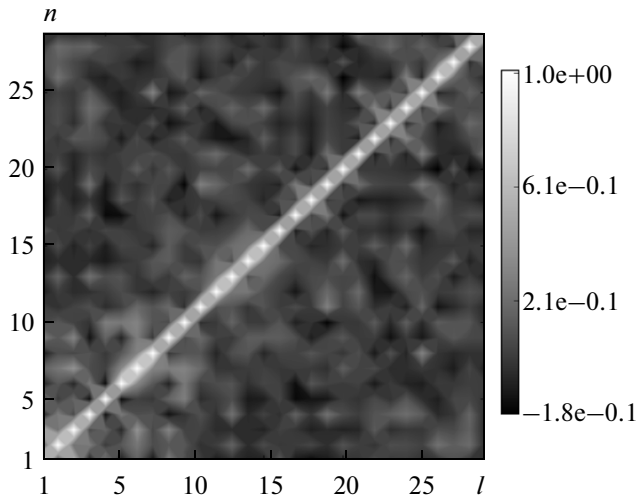

Fig. 5. The correlation coefficient r_{ln} for the geodynamo model.

with close values of l and m[1] (Fig. 7a). At the same time, the spectrum of the magnetic energy has a dense filling within the triangular area of the values of spherical function S_l^m: $l > 0$ $m \le l$ (Fig. 7b). This is due to the inverse cascade of the magnetic energy across the spectrum for the wave numbers m. The cross-helicity spectrum is sign-alternating and its maximal absolute values are concentrated near the diagonal $l = m$ (Fig. 7c), where the product of the spectra S_v, S_b is large.

DISCUSSION

Above, it has been shown that in our dynamo model, the behavior of the geomagnetic dipole is not statistically correlated to the behavior of the small-scale magnetic fields on timescales of hundreds of ka. In the present analysis, we did not consider the probable exchange in the magnetic energy between the dipole and all the other harmonics in the spherical expansion; we only estimated the degree of correlation between the fields with different wave numbers and found this correlation to be extremely low. At the same time, albeit faintly, the behavior of the magnetic dipole still reflects the behavior of the total magnetic energy concentrated in the liquid core. Generally speaking, this is a nontrivial fact because the role of the high harmonics in the turbulent liquid core is very significant, and the above statement is not obvious a priori. However, in order to achieve the dynamo regimes with the realistic values of the inclination, the model should possess strong geostrophy which, in turn, is a source of

[1] The zero values of $l - m$ correspond to the cases when the sign of the spherical function S_l^m does not change along the latitude.

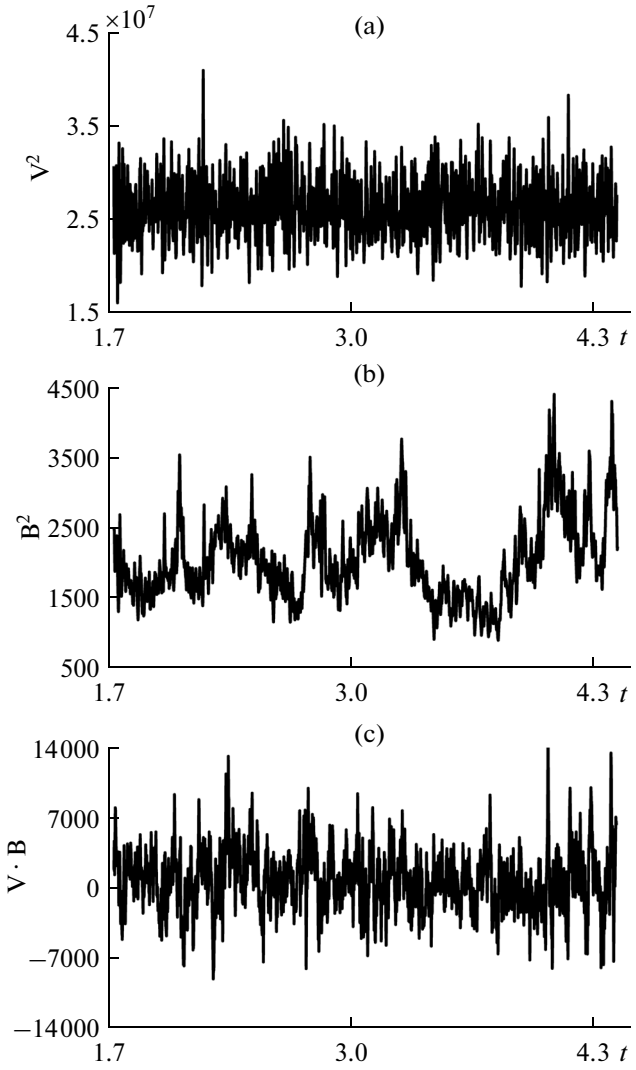

Fig. 6. The evolution of the volume-average (a) V^2, (b) B^2, and (c) cross-helicity.

the preferred role of the dipole magnetic field over the higher harmonics.

The weak dependence of the hydrodynamics in the liquid core on the behavior of the magnetic field during the magnetic reversals and on the magnetic energy overall is another important conclusion. This is due to the fact that the magnetic field favors the force-free configurations for which the direction of the magnetic field is close to the direction of the electric current in the core. The influence of the magnetic field on the flows in the core is a rather fine effect, which is not limited to the trivial suppression of the convection by the magnetic field (Hejda and Reshetnyak, 2010). The structure of the convective cells, which have a shape of cyclones, is largely determined by the purely hydrodynamical factors, namely, the amplitude of the sources of thermal convection, rotational velocity, and hydrodynamic viscosity. In contrast, the configuration of the

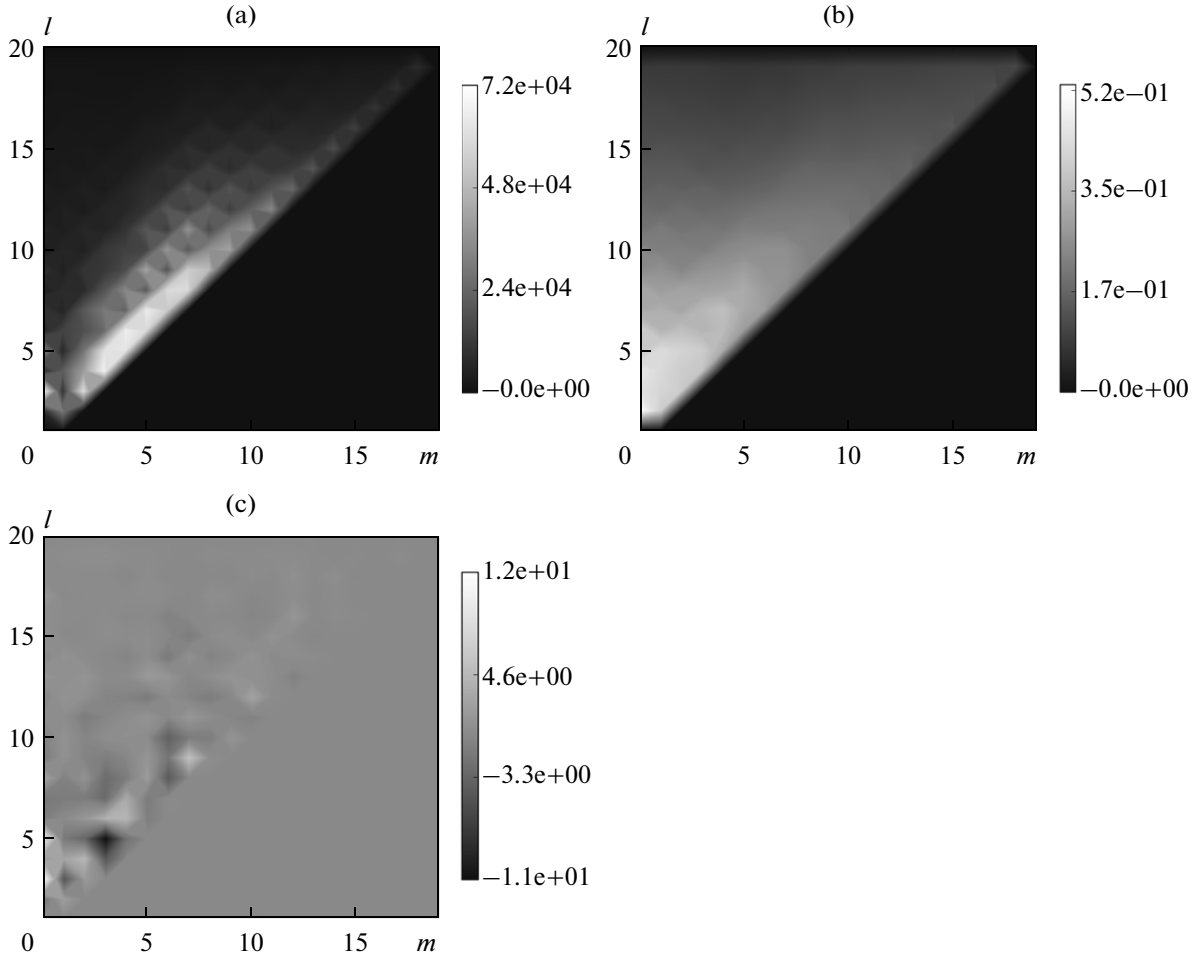

Fig. 7. The 2D spectra of the (a) velocity field S_v, (b) magnetic field S_b, and (c) cross-helicity S_{vb}.

magnetic field is determined by the structure of the velocity field on the scale of its generation and by the fact that the magnetic energy can be transferred from the small scales to the large scales. The latter makes the configuration of the magnetic field barely similar to the velocity field. In contrast to the small scales where the fields **V** and **B** tend to be parallel, the angle between these fields on the large scales can be very significant.

REFERENCES

Bouligand, C., Hulot, G., Khokhlov, A., and Glatzmaier, G.A., Statistical palaeomagnetic field modelling and dynamo numerical simulation, *Geophys. J. Int.*, 2005, vol. 161, pp. 603–626.

Burakov, K.S., Galyagin, D.K., Nachasova, I.E., Reshetnyak, M.Yu., Sokolov, D.D., and Frick, P.G., Wavelet analysis of geomagnetic field intensity for the past 4000 years, *Izv., Phys. Solid Earth*, 1998, vol. 34, no. 9, pp. 773–778.

Christensen, U.R. and Tilgner, A., Power requirement of the geodynamo from ohmic losses in numerical and laboratory dynamos, *Nature*, 2004, vol. 429, pp. 169–171.

Finlay, C.C., Maus, S., Beggan, C.D., Bondar, N.N., Chambodut, A., Chernova, N.A., Chulliat, A., Golovkov, V.P., Hamilton, B., Hamoudi, M., Holme, R., Hulot, G., Kuang, W., Langlais, B., Lesur, V., Lowes, F.J., Luhr, H., Macmillan, S., Mandea, M., McLean, S., Manoj, C., Menvielle, M., Michaelis, I., Olsen, N., Rauberg, J., Rother, M., Sabaka, T.J., Tangborn, A., Toffner-Clausen, L., Thebault, E., Thomson, A.W.P., Wardinski, I., Wei, Z., and Zvereva, T.I., International Geomagnetic Reference Field: the eleventh generation, *Geophys. J. Int.*, 2010, vol. 183, no. 3, pp. 1216–1230. http://www.ngdc.noaa.gov/IAGA/vmod/igrf.html

Hejda, P. and Reshetnyak, M., Nonlinearity in dynamo, *Geophys. Astrophys. Fluid Dyn.*, 2010, vol. 104, no. 6, pp. 25–34.

Hulot, G. and Le Mouël, J-L., A statistical approach to the Earth's main magnetic field, *Phys. Earth Planet. Int.*, 1994, vol. 82, pp. 167–183.

Hulot, G. and Bouligand, C., Statistical palaeomagnetic field modelling and symmetry considerations, *Geophys. J. Int.*, 2005, vol. 161, pp. 591–602.

Hulot, G., Finlay, C.C., Constable, C.G., Olsen, N., and Mandea, M., The magnetic field of planet Earth, *Space Sci. Rev.*, 2010, vol. 152, pp. 159–222.

Jackson, A., Jonkers, A.R.T., and Walker, M.R., Four centuries of geomagnetic secular variation from historical records, *Philos. Trans. R. Soc. London*, 2000, vol. AA58, pp. 957–990. http://jupiter.ethz.ch/~cfinlay/gufm1.html

Khokhlov, A.V., The model of the paleomagnetic secular variations: theory amnd implementation, *Geofiz. Issled.*, 2012, vol. 13, no. 2, pp. 50–61.

Lowes, F.J., Mean-square values on sphere of spherical harmonic on sphere of spherical harmonic vector fields, *J. Geophys. Res.*, 1966, vol. 71, no. 8, p. 2179.

Mauersberger, D., Das Mitel der Energiediche des Geomagnetischen Hauptfeldes an der Erdoberflache und seine Sakulare Anderung, *Gerlands Beitr. Geophys.*, 1956, vol. 65, pp. 207–215.

Parkinson, W.D., *Introduction to Geomagnetism*, Edinburgh: Scottish Acad. Press, 1983.

Rüdiger, G., Kitchatinov, L.L., and Hollerbach, R., *Magnetic Processes in Astrophysics. Theory, Simulations, Experiments*, Weinheim: Wiley-VCH, 2013.

Reshetnyak, M.Yu., Geostrophic balance and reversals of the geomagnetic field, *Rus. J. Earth Sci.*, 2013a, vol. 13, ES1001.

Reshetnyak, M.Yu., *Modelirovanie v geodinamo* (Modeling in Geodynamo), Moscow: Lambert Academic Publishing, 2013b.

Roberts, P.H. and King, E.M., On the genesis of the Earth's magnetism, *Rep. Prog. Phys.*, 2013, vol. 76, 096801.

Woltjer, L., On hydromagnetic equilibrium, *Proc. Natl. Acad. Sci. USA*, 1958, vol. 44, no. 9, pp. 833–841.

Translated by M. Nazarenko

SPELL: 1. hydrodynamical